Correlations and effective interactions in nuclear matter

P. Bożek*
Institute of Nuclear Physics, PL-31-342 Cracow, and Institute of Physics, Rzeszow University, PL-35-959 Rzeszow, Poland

D. J. Dean†
Physics Division, Oak Ridge National Laboratory, P.O. Box 2008, Oak Ridge, Tennessee 37831-6373, USA

H. Müther‡
Institut für Theoretische Physik, Universität Tübingen, D-72076 Tübingen, Germany

(Received 3 April 2006; published 11 July 2006)

We performed self-consistent Green's function calculations for symmetric nuclear matter using realistic nucleon-nucleon (NN) interactions and effective low-momentum interactions ($V_{\mathrm{low}-k}$), which are derived from such realistic NN interactions. We compare the spectral distributions resulting from such calculations. We also introduce a density-dependent effective low-momentum interaction that accounts for the dispersive effects in the single-particle propagator in the medium.

DOI: 10.1103/PhysRevC.74.014303 PACS number(s): 21.30.Fe, 21.65.+f, 24.10.Cn

I. INTRODUCTION

The description of bulk properties of nuclear systems starting from realistic nucleon-nucleon (NN) interactions is a long-standing and unsolved problem. Various models for the NN interaction have been developed, which describe the experimental NN phase shifts up to the threshold for pion production with high accuracy [1–4]. A general feature of all these interaction models are strong short-range and tensor components, which lead to corresponding correlations in the nuclear many-body wave function. Hartree-Fock mean-field theory, which represents the the lowest-order many-body calculations one can perform with such realistic NN interactions, fails to produce bound nuclei [5,6] precisely because Hartree-Fock does not fully incorporate many-body correlation effects.

That correlations beyond the mean field are important is supported by experiments exploring the spectral distribution of the single-particle strength. One experimental fact found in all nuclei is the global depletion of the Fermi sea. A recent experiment from NIKHEF puts this depletion of the proton Fermi sea in ^{208}Pb at a little less than 20% [7] in accordance with earlier nuclear matter calculations [8]. Another consequence of the presence of short-range and tensor correlations is the appearance of high-momentum components in the ground state wave function to compensate for the depleted strength of the mean field. Recent JLab experiments [9] indicate that the amount and location of this strength is consistent with earlier predictions for finite nuclei [10] and calculations of infinite matter [11].

These data and their analysis, however, are not sufficient to allow for a detailed comparison with the predictions derived from the various interaction models at high momenta. In this article, we want to investigate a possibility to separate the predictions for correlations at low and medium momenta, which are constrained by the NN scattering matrix below pion threshold, from the high momentum components, which may strongly depend on the underlying model for the NN interaction. For that purpose we perform nuclear many-body calculations within a model space that allows for the explicit evaluation of low-momentum correlations. The effective Hamiltonian for this model space are constructed from a realistic interaction to account for correlations outside the model space.

This concept of a model space and effective operators appropriately renormalized for this model space has a long history in approaches to the nuclear many-body physics. As an example we mention the effort to evaluate effective operators to be used in Hamiltonian diagonalization calculations of finite nuclei. For a review on this topic see e.g. Ref. [12]. The concept of a model space for the study of infinite nuclear matter was used e.g. by Kuo *et al.* [13–15]. Also the Brueckner-Hartree-Fock (BHF) approximation can be considered as a model-space approach. In this case one restricts the model space to just one Slater determinant and determines the effective interaction through a calculation of the G matrix, the solution of the Bethe-Goldstone equation.

The effective Hamiltonians for such model-space calculations have frequently been evaluated within the Rayleigh-Schrödinger perturbation theory, leading to a non-Hermitian and energy-dependent result. The energy dependence can be removed by considering the so-called folded diagrams as has been discussed e.g. by Brandow [16] and Kuo [17]. We note that the folded-diagram expansion yields effective interaction terms between three and more particle, even if one considers a realistic interaction with two-body terms only [18,19].

During the past few years the folded-diagram technique has been applied to derive an effective low-momentum potential $V_{\mathrm{low}-k}$ [20] from a realistic NN interaction. By construction, $V_{\mathrm{low}-k}$ potentials reproduce the deuteron binding energy, low-energy phase shifts, and the half-on-shell T matrix

*Electronic address: piotr.bozek@ifj.edu.pl
†Electronic address: deandj@ornl.gov
‡Electronic address: herbert.muether@uni-tuebingen.de

calculated from the underlying realistic NN interaction up to the chosen cutoff parameter. The resulting $V_{\mathrm{low}-k}$ turns out to be rather independent of the original NN interaction if this cutoff parameter for the relative momenta is below the value of the pion-production threshold in NN scattering. The off-shell characteristics of the $V_{\mathrm{low}-k}$ effective interaction are not constrained by experimental data and can influence the many-body character of the interaction.

For finite nuclei we find that one does indeed obtain different binding energies for ^{16}O depending on the underlying NN interaction from which one derives the $V_{\mathrm{low}-k}$ interaction. For example, using coupled-cluster techniques at the singles and doubles level (CCSD) [21] we find binding energies for ^{16}O at a lab momentum cutoff of $\Lambda = 2.0$ fm^{-1} to be -143.4 ± 0.4 MeV and -153.3 ± 0.4 MeV for the N^{3}LO [4] and CD-Bonn two-body interactions, respectively. The CCSD calculations were carried out at up to seven major oscillator shells (with extrapolations to an infinite model space) using the intrinsic Hamiltonian defined as $H = T - T_{\mathrm{cm}} + V_{\mathrm{low}-k}$, where T_{cm} is the center-of-mass kinetic energy.

Attractive energies are obtained if such a $V_{\mathrm{low}-k}$ interaction is used in a Hartree-Fock calculation of nuclear matter or finite nuclei [22,23]. High-momentum correlations, which are required to obtain bound nuclear systems from a realistic NN interaction (see above) are taken into account in the renormalization procedure that leads to $V_{\mathrm{low}-k}$. Supplementing these Hartree-Fock calculations with corrections up to third order in the Goldstone perturbation theory leads to results for the ground-state properties of ^{16}O and ^{40}Ca, which are in fair agreement with the empirical data [22]. (One should note that T_{cm} was not included in these calculations.) Calculations in infinite matter demonstrate that $V_{\mathrm{low}-k}$ seems to be quite a good approximation for the evaluation of low-energy spectroscopic data. The results for the pairing derived from the bare interaction are reproduced [23]. The prediction of pairing properties also agree with results obtained phenomenological interactions such as the Gogny force [24,25]. The $V_{\mathrm{low}-k}$ interaction also yields a good approximation for the calculated binding energy of nuclear matter at low densities.

At high densities, however, BHF calculations using $V_{\mathrm{low}-k}$ yield too much binding energy and do not reproduce the saturation feature of nuclear matter [23]. This is because of the fact that $V_{\mathrm{low}-k}$ does not account for the effects of the dispersive quenching of the two-particle propagator, as is done e.g. in the Brueckner G matrix derived from a realistic NN interaction. The saturation can be obtained if a three-nucleon interaction is added to the Hamiltonian [26].

An alternative technique to determine an effective Hamiltonian for a model space calculation is based on a unitary transformation of the Hamiltonian. It has been developed by Suzuki [27] and leads to an energy-independent, Hermitian effective interaction. The unitary-model-operator approach (UMOA) has also been used to evaluate the ground-state properties of finite nuclei [28–31].

In the present study we are going to employ the unitary transformation technique to determine an effective interaction, which corresponds to the $V_{\mathrm{low}-k}$ discussed above. This effective interaction is then used in self-consistent Green's function (SCGF) calculation of infinite nuclear matter. Various groups have recently developed techniques to solve the corresponding equations and determine the energy and momentum distribution of the single-particle strength in a consistent way [11,32–38]. Therefore we can study the correlation effects originating from $V_{\mathrm{low}-k}$ inside the model space and compare it to the correlations derived from the bare interaction. Furthermore, we use the unitary transformation technique to determine an effective interaction which accounts for dispersive effects missing in the original $V_{\mathrm{low}-k}$ (see discussion above).

After this introduction we present the method for evaluating the effective interaction in Sec. II and briefly review the basic features of the SCGF approach in Sec. III. The results of our investigations are presented in Sec. IV, which is followed up by the conclusions.

II. EFFECTIVE INTERACTION

For the definition and evaluation of an effective interaction to be used in a nuclear structure calculation, which is restricted to a subspace of the Hilbert space, the so-called model space, we follow the usual notation and define a projection operator P, which projects onto this model space. The operator projecting on the complement of this subspace is identified by Q and these operators satisfy the usual relations such as $P + Q = 1$, $P^2 = P$, $Q^2 = Q$, and $PQ = 0 = QP$. It is the aim of the UMOA to define a unitary transformation U in such a way that the transformed Hamiltonian does not couple the P and Q space, i.e., $QU^{-1}HUP = 0$.

For a many-body system the resulting Hamiltonian can be evaluated in a cluster expansion, which leads to many-body terms. This is very similar to the folded-diagram expansion, which has been discussed above. In UMOA studies of finite nuclei terms up to three-body clusters have been evaluated [28,29] indicating a convergence of the expansion up to this order.

In the present study we aim to determine an effective two-body interaction and therefore consider two-body systems only. We define the effective interaction as

$$V_{\mathrm{eff}} = U^{-1}(h_0 + v_{12})U - h_0\,, \tag{1}$$

with v_{12} representing the bare NN interaction. The operator h_0 denotes the one-body part of the two-body system and contains the kinetic energy of the interacting particles. This formulation leads to an effective interaction corresponding to $V_{\mathrm{low}-k}$. Because, however, we want to determine an effective interaction of two nucleons in the medium of nuclear matter, we also consider the possibility to add a single-particle potential to h_0. Note that in any case h_0 commutes with the projection operators P and Q.

The operator for the unitary transformation U can be expressed as [39]

$$U = (1 + \omega - \omega^\dagger)(1 + \omega\omega^\dagger + \omega^\dagger\omega)^{-1/2}\,, \tag{2}$$

with an operator ω satisfying $\omega = Q\omega P$ such that $\omega^2 = \omega^{\dagger 2} = 0$. In the following we describe how to determine the matrix elements of this operator ω. As a first step we solve

the two-body eigenvalue equation

$$(h_0 + v_{12})|\Phi_k\rangle = E_k|\Phi_k\rangle\,. \tag{3}$$

This can be done separately for each partial wave of the two-nucleon problem. Partial waves are identified by total angular momentum J, spin S, and isospin T. The relative momenta are appropriately discretized such that we can reduce the eigenvalue problem to a matrix diagonalization problem. Momenta below the cutoff momentum Λ define the P space and will subsequently be denoted by $|p\rangle$ and $|p'\rangle$. Momenta representing the Q space are labeled $|q\rangle$ and $|q'\rangle$, whereas states $|i\rangle$, $|j\rangle$, $|k\rangle$, and $|l\rangle$ refer to basis states of the total $P+Q$ space.

From the eigenstates $|\Phi_k\rangle$ we determine those N_P (N_P denoting the dimension of the P space) eigenstates $|\Phi_p\rangle$, which have the largest overlap with the P space and determine

$$\langle q|\omega|p'\rangle = \sum_{p=1}^{N_P}\langle q|Q|\Phi_p\rangle\langle\tilde{\varphi}_p|p'\rangle, \tag{4}$$

with $|\varphi_p\rangle = P|\Phi_p\rangle$ and $\langle\tilde{\varphi}_p|$ denoting the biorthogonal state, satisfying

$$\sum_p\langle\tilde{\varphi}_k|p\rangle\langle p|\varphi_{k'}\rangle = \delta_{k,k'} \quad \text{and} \quad \sum_k\langle p'|\tilde{\varphi}_k\rangle\langle\varphi_k|p\rangle = \delta_{p,p'}\,. \tag{5}$$

In the next step we solve the eigenvalue problem in the P space

$$\omega^\dagger\omega|\chi_p\rangle = \mu_p^2|\chi_p\rangle \tag{6}$$

and use the results to define

$$|\nu_p\rangle = \frac{1}{\mu_p}\omega|\chi_p\rangle, \tag{7}$$

which because of the fact that $\omega = Q\omega P$ can be written as

$$\langle q|\nu_p\rangle = \frac{1}{\mu_p}\sum_{p'}\langle q|\omega|p'\rangle\langle p'|\chi_p\rangle. \tag{8}$$

Using Eqs. (6)–(8) and the representation of U in Eq. (2), the matrix elements of the unitary transformation operator U can be written

$$\begin{aligned}
\langle p''|U|p'\rangle &= \langle p''|(1+\omega^\dagger\omega)^{-1/2}|p'\rangle \\
&= \sum_{p=1}^{N_P}\left(1+\mu_p^2\right)^{-1/2}\langle p''|\chi_p\rangle\langle\chi_p|p'\rangle\,, \qquad (9)\\
\langle q|U|p'\rangle &= \langle q|\omega(1+\omega^\dagger\omega)^{-1/2}|p'\rangle \\
&= \sum_{p=1}^{N_P}\left(1+\mu_p^2\right)^{-1/2}\mu_p\langle q|\nu_p\rangle\langle\chi_p|p'\rangle, \qquad (10)\\
\langle p'|U|q\rangle &= -\langle p'|\omega^\dagger(1+\omega\omega^\dagger)^{-1/2}|q\rangle \\
&= -\sum_{p=1}^{N_P}\left(1+\mu_p^2\right)^{-1/2}\mu_p\langle p'|\chi_p\rangle\langle\nu_p|q\rangle\,, \qquad (11)\\
\langle q'|U|q\rangle &= \langle q'|(1+\omega\omega^\dagger)^{-1/2}|q\rangle \\
&= \sum_{p=1}^{N_P}\left\{\left(1+\mu_p^2\right)^{-1/2}-1\right\}\langle q'|\nu_p\rangle\langle\nu_p|q\rangle + \delta_{q,q'}\,. \qquad (12)
\end{aligned}$$

These matrix elements of U can then be used to determine the matrix elements of the effective interaction $V_{\rm eff}$ according to Eq. (1). They might also be used to define matrix elements of other effective operators.

III. SELF-CONSISTENT GREEN'S FUNCTION APPROACH

One of the key quantities within the SCGF approach is the retarded single-particle (sp) Green's function or sp propagator $G(k,\omega)$ (see e.g. Ref. [40]). Its imaginary part can be used to determine the spectral function

$$A(k,\omega) = -2\,\mathrm{Im}\,G(k,\omega+\mathrm{i}\eta)\,. \tag{13}$$

The spectral function provides the information about the energy and momentum distribution of the single-particle strength, i.e., the probability for adding or removing a particle with momentum k and leaving the residual system at an excitation energy related to ω. In the limit of the mean-field or quasiparticle approximation the spectral function is represented by a δ function and takes the simple form

$$A(k,\omega) = 2\pi\,\delta(\omega-\varepsilon_k)\,, \tag{14}$$

with the quasiparticle energy ε_k for a particle with momentum k. The sp Green's function can be obtained from the solution of the Dyson equation, which reduces for the system of homogeneous infinite matter to a a simple algebraic equation

$$\left[\omega - \frac{k^2}{2m} - \Sigma(k,\omega)\right]G(k,\omega) = 1\,, \tag{15}$$

where $\Sigma(k,\omega)$ denotes the complex self-energy. The self-energy can be decomposed into a generalized Hartree-Fock part plus a dispersive contribution

$$\Sigma(k,\omega) = \Sigma^{\rm HF}(k) - \frac{1}{\pi}\int_{-\infty}^{+\infty}d\omega'\frac{\mathrm{Im}\Sigma(k,\omega'+\mathrm{i}\eta)}{\omega-\omega'}. \tag{16}$$

The next step is to obtain the self-energy in terms of the in-medium two-body scattering T matrix. It is possible to express $\mathrm{Im}\Sigma(k,\omega+\mathrm{i}\eta)$ in terms of the retarded T matrix [11,41,42] (for clarity, spin- and isospin quantum numbers are suppressed)

$$\begin{aligned}
\mathrm{Im}\Sigma(k,\omega+\mathrm{i}\eta) = \frac{1}{2}\int\frac{d^3k'}{(2\pi)^3}\int_{-\infty}^{+\infty}\frac{d\omega'}{2\pi} \\
\times\langle\mathbf{kk}'|\mathrm{Im}T(\omega+\omega'+\mathrm{i}\eta)|\mathbf{kk}'\rangle \\
\times[f(\omega')+b(\omega+\omega')]A(k',\omega'). \qquad (17)
\end{aligned}$$

Here and in the following $f(\omega)$ and $b(\omega)$ denote the Fermi and Bose distribution functions, respectively. These functions depend on the chemical potential μ and the inverse temperature β of the system. Note, that the results discussed below are for the limit of zero temperature. The in-medium scattering matrix T is to be determined as a solution of the integral equation

$$\begin{aligned}
\langle\mathbf{kk}'|T(\Omega+\mathrm{i}\eta)|\mathbf{pp}'\rangle = \langle\mathbf{kk}'|V|\mathbf{pp}'\rangle + \int\frac{d^3q\,d^3q'}{(2\pi)^6} \\
\times\langle\mathbf{kk}'|V|\mathbf{qq}'\rangle G_{\rm II}^0(\mathbf{qq}',\Omega+i\eta) \\
\times\langle\mathbf{qq}'|T(\Omega+\mathrm{i}\eta)|\mathbf{pp}'\rangle\,, \qquad (18)
\end{aligned}$$

where

$$G^0_{\rm II}(k_1,k_2,\Omega+i\eta)=\int_{-\infty}^{+\infty}\frac{d\omega}{2\pi}\int_{-\infty}^{+\infty}\frac{d\omega'}{2\pi}A(k_1,\omega)\times A(k_2,\omega')\frac{1-f(\omega)-f(\omega')}{\Omega-\omega-\omega'+i\eta}. \quad (19)$$

stands for the two-particle Green's function of two noninteracting but dressed nucleons. The matrix elements of the two-body interaction V represent either the bare NN interaction v_{12} or the effective interaction $V_{\rm eff}$, in which case the integrals are cut at the cutoff parameter Λ.

The in-medium scattering equation (18) can be reduced to a set of one-dimensional integral equations if the two-particle Green's function in Eq. (19) is written as a function of the total and relative momenta of the interacting pair of nucleons and the usual angle-average approximation is employed (see e.g. Ref. [43] for the accuracy of this approximation). This leads to integral equations in the usual partial waves, which can be solved very efficiently if the two-body interaction is represented in terms of separable interaction terms of a sufficient rank [33].

Finally, we consider the generalized Hartree-Fock contribution to the self-energy in Ref. (16), which takes the form

$$\Sigma^{\rm HF}(k)=\int\frac{d^3k'}{(2\pi)^3}\langle\mathbf{k},\mathbf{k}'|V|\mathbf{k},\mathbf{k}'\rangle n(k'), \quad (20)$$

where $n(k)$ is the correlated momentum distribution, which is to be calculated from the spectral function by

$$n(k)=\int_{-\infty}^{+\infty}\frac{d\omega}{2\pi}f(\omega)A(k,\omega). \quad (21)$$

Also the energy per particle, E/A, can be calculated from the spectral function using Koltun's sum rule

$$\frac{E}{A}=\frac{1}{\rho}\int\frac{d^3k}{(2\pi)^3}\int_{-\infty}^{+\infty}\frac{d\omega}{2\pi}\frac{1}{2}\left(\frac{k^2}{2m}+\omega\right)A(k,\omega)f(\omega). \quad (22)$$

Eqs. (13)–(21) define the so-called T-matrix approach to the SCGF equations. They form a symmetry conserving approach in the sense of Ref. [42], which means that thermodynamical relations such as the Hughenholtz-Van Hove theorem [33,44] are obeyed.

The BHF approximation, which is very popular in nuclear physics, can be regarded as a simple approximation to this T-matrix approach. In the BHF approximation one reduces the spectral function $A(k,\omega)$ to the quasiparticle approximation (14). Furthermore one ignores the hole-hole scattering terms in the scattering Eq. (18), which means that one replaces

$$[1-f(\omega)-f(\omega')] \quad\rightarrow\quad [1-f(\omega)][1-f(\omega')], \quad (23)$$

which is the usual Pauli operator. This reduces the in-medium scattering equation to the Bethe-Goldstone equation. The removal of the hole-hole scattering terms leads to real self-energies $\Sigma(k,\omega)$ at energies ω below the chemical potential, i.e., for the hole states.

IV. RESULTS AND DISCUSSION

In the following we discuss results for symmetric nuclear matter obtained from SCGF calculations. These calculations are either performed in the complete Hilbert space using the bare CD-Bonn [1] interaction or in the model space, which is defined by a cutoff parameter $\Lambda = 2$ fm^{-1} in the two-body scattering equation, employing the corresponding effective interaction $V_{{\rm low}-k}$, which is derived from the CD-Bonn interaction using the techniques described in Sec. II. We note that using this unitary model operator technique we were able to reproduce the results of the BHF calculations presented in Ref. [23], which used tabulated matrix elements of Ref. [20] with good accuracy. The NN interaction has been restricted to partial waves with total angular momentum J less than 6.

Results for the calculated energy per nucleon are displayed in Fig. 1 for various densities, which are labeled by the corresponding Fermi momentum k_F. The effective interaction $V_{{\rm low}-k}$ accounts for a considerable fraction of the short-range NN correlations, which are induced by realistic interactions such as the CD-Bonn interactions. Therefore, already the Hartree-Fock approximation using this $V_{{\rm low}-k}$ yields reasonable results for the energies as can be seen from the dotted line of Fig. 1. Hartree-Fock calculations using the bare CD-Bonn interaction yield positive energies ranging between 2–15 MeV/c for the densities considered in this figure. Note that the CD-Bonn interaction should be considered as a soft realistic interaction. Interaction models, which are based on local potentials, such as the Argonne interaction [2], yield more repulsive Hartree-Fock energies [6].

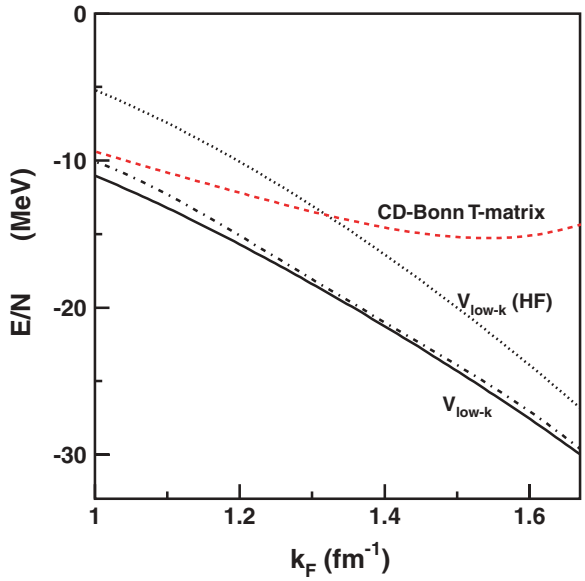

FIG. 1. (Color online) Binding energy per nucleon for symmetric nuclear matter as function of the Fermi momentum: Results of self-consistent T-matrix calculations for the CD-Bonn potential (dashed line), are compared to results of calculations using $V_{{\rm low}-k}$ with $\Lambda = 2\,{\rm fm}^{-1}$ in the Hartree-Fock approximation (dotted line), the self-consistent second order approximation (dashed-dotted line) and for the self-consistent T-matrix approximation (solid line) within the model space.

The inclusion of correlations within the model space yields a substantial decrease of the energy. The self-consistent T-matrix approach provides additional attraction ranging between 6 MeV/c at a density of 0.4 ρ_0 (with ρ_0 the empirical saturation density) and 3 MeV/c at 2 ρ_0. The fixed cutoff parameter Λ seems to reduce the phasespace available for correlations beyond the mean-field approach at higher densities. Therefore the energy calculated in the self-consistent T-matrix approach reduces to the Hartree-Fock result at large densities.

Figure 1 also displays the energies resulting from a SCGF calculation within the model space, in which the T-matrix has been approximated by the corresponding scattering matrix including only terms up to second order in the NN interaction V. The results of such second-order calculations in $V_{\mathrm{low}-k}$ are represented by the dashed-dotted line and show a very good agreement with the model-space calculations including the full T matrix. This confirms the validity of approaches, which consider correlation effects within the model space in a perturbative way.

All these model space calculations using $V_{\mathrm{low}-k}$, however, fail to reproduce the results of the SCGF calculations, which are obtained in the complete space using the bare NN interaction, which are labeled by CD Bonn T matrix in Fig. 1. In particular, the model-space calculations yield too-attractive energies at high densities and therefore do not exhibit a minimum for the energy as a function of density. This confirms the results of the BHF calculations of Ref. [23].

It has been argued [23] that this overestimate of the binding energy at high densities is because of the fact that $V_{\mathrm{low}-k}$ does not account for the quenching of correlation effects, which is because of the Pauli principle and the dispersive effects in the single-particle propagator getting more important with increasing density. Therefore we try to account for the dispersive quenching effects by adopting the following two-step procedure.

In a vein similar to the use of a G matrix within a self-consistent BHF calculation, as a first step we perform BHF calculations using $V_{\mathrm{low}-k}$. The resulting single-particle spectrum is approximated by an effective mass parametrization. This parametrization of the mean field is employed to define the single-particle operator h_0, used in Eq. (1) and the following equations of Sec. II (see also Ref. [30]). The resulting effective interaction is used again for a BHF calculation within the model space, leading to an update of the mean-field parametrization. The procedure is repeated until a self-consistent result is obtained. This leads to effective masses ranging between $m^*/m = 0.86$ for a Fermi momentum k_F of 1 fm^{-1} and $m^*/m = 0.61$ for a Fermi momentum k_F of 1.7 fm^{-1}. Because these mean-field parametrizations depend on the density, this method yields an effective density-dependent interaction, which in the limit of the density $\rho \to 0$ coincides with $V_{\mathrm{low}-k}$. Therefore we call this effective interaction the density-dependent $V_{\mathrm{low}-k}$ or, in short, $V_{\mathrm{low}-k}(\rho)$. Such a procedure amounts to summing up certain higher order terms in the full many-body problem.

In a second step this $V_{\mathrm{low}-k}(\rho)$ is used in SCGF calculations at the corresponding density. Energies resulting from such model-space calculations using $V_{\mathrm{low}-k}(\rho)$ are presented in Fig. 2. The comparison of the various calculations within the model space exhibits the same features as discussed above for the original $V_{\mathrm{low}-k}$. The correlation within the model space provide a substantial reduction of the energy as can be seen from the comparison of the self-consistent T-matrix approach with the Hartree-Fock results. The approach treating correlations up to second order in $V_{\mathrm{low}-k}(\rho)$ yields energies that are very close to the complete T-matrix approach.

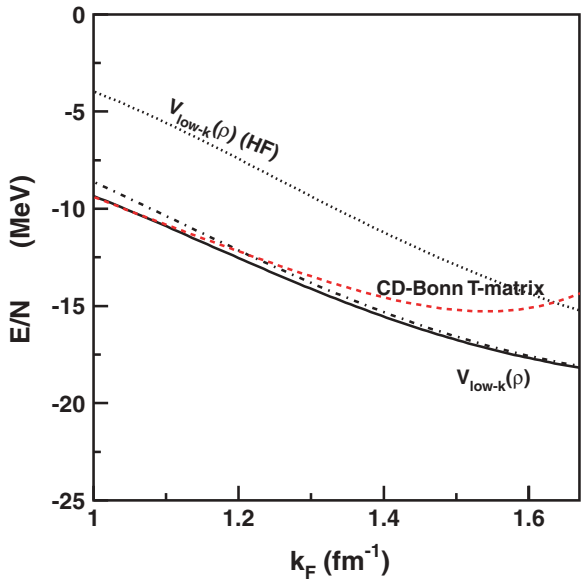

FIG. 2. (Color online) Same as Fig. 1 but for $V_{\mathrm{low}-k}(\rho)$ calculated at each density.

The density dependence of the effective interaction $V_{\mathrm{low}-k}(\rho)$ yields a significant improvement for the comparison between the model-space calculations and the SCGF calculation using the bare CD-Bonn interaction. Note that the energy scale has been adjusted going from Fig. 1 to Fig. 2. The discrepancy remaining at densities above ρ_0 might be because of the effects of the Pauli quenching, which are not included in $V_{\mathrm{low}-k}(\rho)$. Using the UMOA techniques these Pauli effects would be included in terms of effective three-nucleon forces. These deviations could also originate from the simple parametrization of the dispersive quenching in $V_{\mathrm{low}-k}(\rho)$.

Our investigations also provide the possibility to explore the effects of correlations evaluated within the model space using the effective interaction $V_{\mathrm{low}-k}$. We can furthermore compare these correlation effects with the corresponding effects determined by the bare interaction in the unrestricted space. As a first example, we discuss the imaginary part of the self-energy calculates at the empirical saturation density ρ_0 for various nucleon momenta p as displayed in Fig. 3. The calculations within the model space reproduce the results of the unrestricted calculations with a good accuracy in the energy interval for ω ranging between 50 MeV below and 50 MeV above the chemical potential μ. The remaining differences around the Fermi energy can be attributed to the difference in the effective masses obtained using the $V_{\mathrm{low}-k}$ and the bare potential [45]. The agreement between the T-matrix results around $\omega = \mu$ using the two potentials is improved if one rescales by the ratio of the effective masses. The imaginary

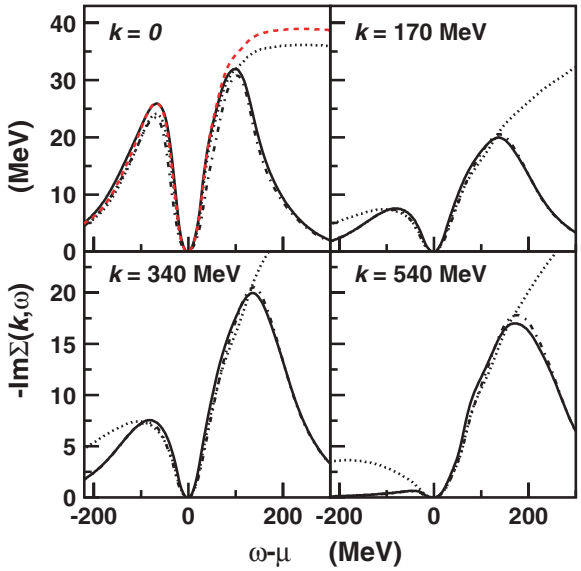

FIG. 3. (Color online) Imaginary part of the self-energy as a function of the energy ω for various momenta p as indicated in the panels [see Eq. (17)]. The results have been determined for the empirical saturation density ρ_0; using $V_{\text{low}-k}$ in the T-matrix approximation (solid line), using $V_{\text{low}-k}$ in the second-order approximation (dashed-dotted line), and employing CD-Bonn interaction in the T-matrix approximation (dotted line). The dashed line in the first panel denotes the results of the T-matrix calculation with the CD-Bonn potential rescaled by the ratio of the effective masses at the Fermi momentum obtained with the $V_{\text{low}-k}$ and the bare CD-Bonn potential.

part calculated with $V_{\text{low}-k}$, however, is much smaller than the corresponding result obtained for the bare interaction at energies $\omega - \mu$ above 100 MeV. Furthermore the model-space calculations do not reproduce the imaginary part for energies below the chemical potential at momenta k above 400 MeV/c.

The imaginary part of the self-energy is a very important ingredient for the evaluation of the spectral function $A(k, \omega)$ and therefore also for the calculation of the occupation probability $n(k)$ [see Eq. (21)]. The small values for the imaginary part of the self-energy at high momenta k and negative energies $\omega - \mu$ leads to occupation probabilities at these momenta, which are much smaller than the corresponding predictions derived from bare realistic NN interactions, as can be seen from Fig. 4. This missing strength in the prediction of $V_{\text{low}-k}$ at high momenta is accompanied by larger occupation probabilities at low momenta. The self-consistent T-matrix approximation using CD-Bonn yields an occupation probability at $k = 0$ of 0.897, whereas the corresponding number using $V_{\text{low}-k}$ is 0.920. For this comparison one must keep in mind that this reduction of the occupation probability $n(k = 0)$ using $V_{\text{low}-k}$ reflects only the effects that are the result of correlations within the model space. Correlation effects because of configurations outside the model space could be accounted for by a renormalization of the single-particle density operator employing the same unitary transformation that has been used to define the effective interaction $V_{\text{low}-k}$.

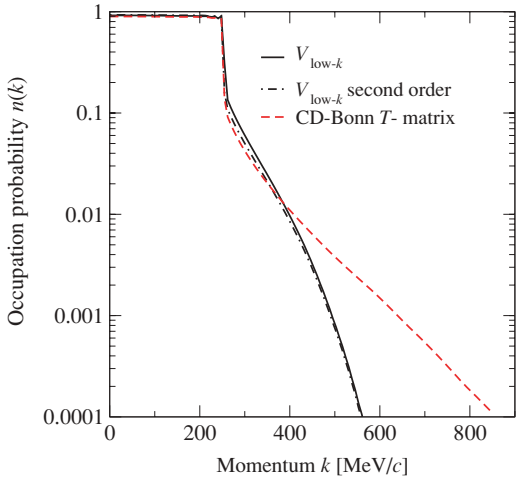

FIG. 4. (Color online) Momentum distribution $n(k)$ [see Eq. (21)] calculated for nuclear matter at the empirical saturation density ρ_0. Results of the T-matrix approximation within the model space (solid line) are compared to results of the second-order approximation (dashed-dotted line) and the T-matrix approximation (dotted line) in the unrestricted space.

At this density, the calculation including only terms up to second order in $V_{\text{low}-k}$ yields a rather good approximation to the self-consistent T-matrix approximation within the model space.

As a second example we consider the imaginary part of the self-energy calculated at a lower density $\rho = 0.4 \times \rho_0$. The results displayed in Fig. 5 refer to nucleons with momentum $k = 0$. Also at this density we find that the imaginary part evaluated with $V_{\text{low}-k}$ drops to zero at large positive energies much faster than the predictions derived from the bare interaction (see upper panel on the left in Fig. 5).

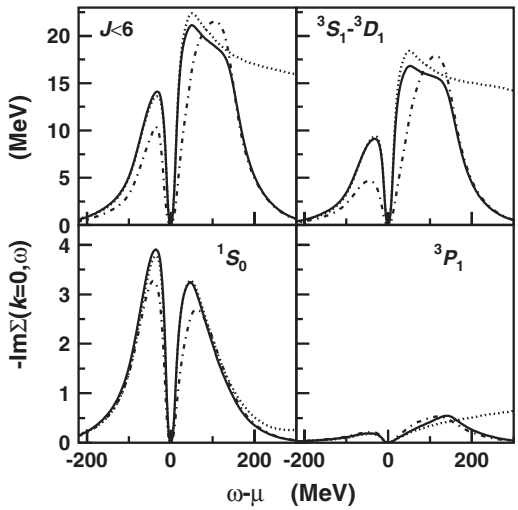

FIG. 5. Imaginary part of the self-energy as a function of the energy ω for nucleons with momentum $k = 0$ calculated at the density $\rho = 0.4 \times \rho_0$. Results of the T-matrix approach (solid line) and the second-order approximation (dashed-dotted line) within the model space are compared to results obtained in the unrestricted calculation (dotted line).

It is worth noting that at this low density the second-order approximation is not such a good approximation to the full T-matrix approach as it is for the higher densities. Characteristic differences between the dashed-dotted and the solid line show up at energies ω close to the chemical potential. To trace the origin of these differences we display in Fig. 5 the contributions of various partial waves of NN interaction channels to this imaginary part. It turns out that the differences are largest in the $^3S_1 - {}^3D_1$ and the $^1S_0$ channels. This means that the perturbative approach is not very successful in those two channels that tend to form quasibound states. In these channels all particle-particle hole-hole ladders have to be summed up to obtain the pairing solution. Note that the pairing solutions are suppressed at higher densities if the effects of short-range correlations are properly taken into account [46,47].

Furthermore, we point out that a different scale is used in the two lower panels of Fig. 5. Taking this into account, it is evident from this figure that the main contribution to the imaginary part of the self-energy, and that means the main contribution to the character of the deviation of the spectral function from the mean-field approach, originates from the NN interaction in the $^3S_1 - {}^3D_1$ channel.

V. CONCLUSIONS

During the past few years it has become very popular to perform nuclear structure calculations using effective low-momentum NN interactions. These $V_{\mathrm{low}-k}$ interactions are based on a realistic model of the NN interaction. They are constructed to be different from zero only within a model space defined by a cutoff Λ in the relative momenta of the interacting nucleons. Within this model space they reproduce the NN data of the underlying bare interaction, although the many-body solutions may show differences with different starting NN interactions.

For this study we performed SCGF calculations of symmetric nuclear matter employing $V_{\mathrm{low}-k}$ effective interactions as well as the bare CD-Bonn interaction they are based on. Special attention was paid to the correlations that can be described within this model space as compared to correlations predicted by the underlying interaction within the unrestricted space.

Using a cutoff $\Lambda = 2$ fm^{-1} we find that the spectral distribution of the single-particle strength in an energy window of ± 50 MeV around the Fermi energy is rather well reproduced by the calculation using $V_{\mathrm{low}-k}$. The effective interaction $V_{\mathrm{low}-k}$ is softer than typical realistic NN interactions. Therefore for many observables it is sufficient to approximate the full in-medium scattering matrix T by the approximation including terms up to second order in $V_{\mathrm{low}-k}$. This justifies the use of the resummed effective interaction in many-body approximations that do not include ladder-diagram resummation. Special attention must be paid to nuclear systems at smaller densities: the possible formation of quasibound states may require the nonperturbative treatment of the NN scattering in the medium. This also has implications for the use of $V_{\mathrm{low}-k}$ in studies of weakly bound nuclear systems.

The model-space approach cannot reproduce correlation effects, which lead to spectral strength at high energies and high momenta. For nuclear matter at the empirical saturation density ρ_0 the momentum distribution is reliably predicted up to a momentum of 400 MeV/c. This could be improved by a renormalization of the single-particle density operator.

The $V_{\mathrm{low}-k}$ approach overestimates the binding energy per nucleon at high densities. Therefore we introduced a density-dependent effective interaction $V_{\mathrm{low}-k}(\rho)$ that we constructed along the same line as the original $V_{\mathrm{low}-k}$. The new effective interaction accounts for a dispersive correction of the single-particle propagator in the medium. This improves the behavior of the effective interaction significantly. For densities above ρ_0, however, the binding energies calculated with $V_{\mathrm{low}-k}(\rho)$ are still too large. This might be improved by determining effective three-nucleon forces explicitly from the underlying bare interaction. Note, however, that other three-nucleon forces, representing e.g. the relativistic effects included in a Dirac-Brueckner-Hartree-Fock calculation or subnucleonic degrees of freedom, might be required to reproduce the empirical saturation point of nuclear matter.

ACKNOWLEDGMENTS

This work is supported in part by the Polish State Committee for Scientific Research grant 2P03B05925U.S; the Department of Energy under contract DE-AC05-00OR22725 with UT-Battelle, LLC (Oak Ridge National Laboratory); and the Deutsche Forschungsgemeinschaft (SFB 382).

[1] R. Machleidt, F. Sammarruca, and Y. Song, Phys. Rev. C **53**, R1483 (1996).
[2] R. B. Wiringa, V. G. J. Stoks, and R. Schiavilla, Phys. Rev. C **51**, 38 (1995).
[3] V. G. J. Stoks, R. A. M. Klomp, C. P. F. Terheggen, and J. J. de Swart, Phys. Rev. C **49**, 2950 (1994).
[4] D. R. Entem and R. Machleidt, Phys. Rev. C **68**, 041001(R) (2003).
[5] H. Müther and A. Polls, Prog. Part. Nucl. Phys. **45**, 243 (2000).
[6] H. Müther and A. Polls, Phys. Rev. C **61**, 014304 (2000).
[7] M. F. van Batenburg, Ph.D. thesis, University of Utrecht, 2001.
[8] B. E. Vonderfecht, W. H. Dickhoff, A. Polls, and A. Ramos, Phys. Rev. C **44**, R1265 (1991).
[9] D. Rohe *et al.*, Phys. Rev. Lett. **93**, 182501 (2004).
[10] H. Müther and W. H. Dickhoff, Phys. Rev. C **49**, R17 (1994).
[11] T. Frick and H. Müther, Phys. Rev. C **68**, 034310 (2003).
[12] D. J. Dean, T. Engeland, M. Hjorth-Jensen, M. Kartamychev, and E. Osnes, Prog. Part. Nucl. Phys. **53**, 419 (2004).
[13] Z. Y. Ma and T. T. S. Kuo, Phys. Lett. **B127**, 137 (1983).
[14] H. Q. Song and T. T. S. Kuo, Phys. Rev. C **43**, 2883 (1991).
[15] T. T. S. Kuo and Y. Tzeng, Int. J. Mod. Phys. E **3**, 523 (1994).

[16] B. H. Brandow, Rev. Mod. Phys. **39**, 771 (1967).
[17] T. T. S. Kuo, S. Y. Lee, and K. F. Ratcliff, Nucl. Phys. **A176**, 65 (1971).
[18] A. Polls, H. Müther, A. Faessler, T. T. S. Kuo, and E. Osnes, Nucl. Phys. **A401**, 124 (1983).
[19] H. Müther, A. Polls, and T. T. S. Kuo, Nucl. Phys. **A435**, 548 (1985).
[20] S. K. Bogner, T. T. S. Kuo, and A. Schwenk, Phys. Rep. **386**, 1 (2003).
[21] D. J. Dean and M. Hjorth-Jensen, Phys. Rev. C **69**, 054320 (2004).
[22] L. Coraggio, N. Itaco, A. Covello, A. Gargano, and T. T. S. Kuo, Phys. Rev. C **68**, 034320 (2003).
[23] J. Kuckei, F. Montani, H. Müther, and A. Sedrakian, Nucl. Phys. **A723**, 32 (2003).
[24] J. Decharge and D. Gogny, Phys. Rev. C **21**, 1568 (1980).
[25] A. Sedrakian, T. T. S. Kuo, H. Müther, and P. Schuck, Phys. Lett. **B576**, 68 (2003).
[26] S. K. Bogner, A. Schwenk, R. J. Furnstahl, and A. Nogga, Nucl. Phys. **A763**, 59 (2005).
[27] K. Suzuki, Prog. Theor. Phys. **68**, 246 (1982).
[28] K. Suzuki and R. Okamoto, Prog. Theor. Phys. **92**, 1045 (1994).
[29] H. Kumagai, K. Suzuki, and R. Okamoto, Prog. Theor. Phys. **97**, 1023 (1997).
[30] S. Fujii, R. Okamoto, and K. Suzuki, Phys. Rev. C **69**, 034328 (2004).
[31] R. Roth, P. Papakonstantinou, N. Paar, H. Hergert, T. Neff, and H. Feldmeier, Phys. Rev. C **73**, 044312 (2006).
[32] P. Bożek and P. Czerski, Eur. Phys. J. A **11**, 271 (2001).
[33] P. Bożek, Phys. Rev. C **65**, 054306 (2002).
[34] P. Bożek, Eur. Phys. J. A **15**, 325 (2002).
[35] Y. Dewulf, D. Van Neck, and M. Waroquier, Phys. Rev. C **65**, 054316 (2002).
[36] Y. Dewulf, W. H. Dickhoff, D. Van Neck, E. R. Stoddard, and M. Waroquier, Phys. Rev. Lett. **90**, 152501 (2003).
[37] W. H. Dickhoff and E. P. Roth, Acta Phys. Pol. B **33**, 65 (2002); E. P. Roth, Ph.D. thesis, Washington University, St. Louis, 2000.
[38] T. Frick, H. Müther, A. Rios, A. Polls, and A. Ramos, Phys. Rev. C **71**, 014313 (2005).
[39] K. Suzuki, Prog. Theor. Phys. **68**, 246 (1982).
[40] W. H. Dickhoff and D. Van Neck, *Many-Body Theory Exposed!* (World Scientific, Singapore, 2005).
[41] P. Bożek, Phys. Rev. C **59**, 2619 (1999).
[42] L. P. Kadanoff and G. Baym, *Quantum Statistical Mechanics* (Benjamin, New York, 1962).
[43] E. Schiller, H. Müther, and P. Czerski, Phys. Rev. C **59**, 2934 (1999).
[44] N. M. Hugenholtz and L. Van Hove, Physica **24**, 363 (1958).
[45] W. H. Dickhoff, Phys. Rev. C **58**, 2807 (1998).
[46] P. Bożek, Phys. Lett. **B551**, 93 (2003).
[47] H. Müther and W. H. Dickhoff, Phys. Rev. C **72**, 054313 (2005).